



# Dynamic performances of adsorbents in an industrial-sized packed bed column for lead ion removal

Mohd Hardyanto Vai Bahrun<sup>1</sup> · Awang Bono<sup>2</sup> · Muhammad Abbas Ahmad Zaini<sup>1,3</sup> · Norasikin Othman<sup>1,3</sup> · Agus Saptoro<sup>4</sup>

Received: 19 May 2022 / Revised: 23 September 2022 / Accepted: 9 October 2022 / Published online: 15 October 2022  
© The Author(s), under exclusive licence to Springer-Verlag GmbH Germany, part of Springer Nature 2022

## Abstract

The dynamic performances of various adsorbents in removing lead ion, Pb(II), from aqueous solution in an industrial-sized packed bed column were investigated through numerical simulation, by employing a linear driving force (LDF) approximation model in Aspen Adsorption simulation tool. The size of the real implemented packed bed column with dimensions of 0.9730 m height and 0.6096 m diameter, with a design flowrate of 631 mL/s and inlet concentration of 0.1 mg/L Pb(II) aqueous solution, was used to represent an industrial-sized packed bed column. Here, the dynamic performances of ten Langmuir-fitted adsorbents for removing Pb(II) from an aqueous solution were evaluated. Among the ten adsorbents, the apricot stone AC gave the highest dynamic adsorptive performance with the highest saturation time (203 days) and percentage removal (95.6%). This suggests a cheaper and environmental-friendly alternative of using biomass-activated adsorbent. Based on the simulation results of the ten adsorbents, a simple analysis method was formulated as a preliminary screening for comparing the adsorptive performance using information from the batch experiments related to separation factor and total adsorbent mass. The Langmuir separation factor,  $R_L$ , can be used as a preliminary indicator to rank various adsorbents in removing Pb(II). In the case of available adsorbent density, the  $m_{\text{total}}$  indicator is more reliable and gives a better indicator than  $R_L$ . This present paper provides a preliminary screening in comparing various adsorbents' performance operated in a packed bed column, especially the industrial-sized packed bed column.

**Keywords** Aspen Adsorption · Dynamic analysis · Industrial-sized column · Langmuir · Simulation

## 1 Introduction

Environmental pollution is one of the most serious problems faced by humanity and other life forms on our planet today. Urbanization, industrialization, economic development, and overpopulation have contributed to the increase in energy consumption and waste discharges [1, 2]. Improper management of waste discharges leads to various types of environmental pollution. Environmental pollution can be defined as the contamination of the physical and biological components of the Earth or atmosphere system to such an extent that normal environmental processes are adversely affected [3]. And, one of the major contaminations found is heavy metals.

Contaminations of hazardous metals into the aquatic environment are a worldwide concern because they have caused severe and persistent hazardous problems in different domains of the environment. For example, lead commonly exists in industrial and agricultural

✉ Awang Bono  
awangbono@gmail.com

<sup>1</sup> School of Chemical and Energy Engineering, Faculty of Engineering, Universiti Teknologi Malaysia, UTM, 81310 Johor Bahru, Johor, Malaysia

<sup>2</sup> GRISM Innovative Solutions, Kota Kinabalu, Sabah, Malaysia

<sup>3</sup> Centre of Lipids Engineering and Applied Research (CLEAR), Ibnu Sina Institute for Scientific and Industrial Research (ISI-SIR), Universiti Teknologi Malaysia, UTM, 81310 Johor Bahru, Johor, Malaysia

<sup>4</sup> Department of Chemical and Energy Engineering, Faculty of Engineering and Science, Curtin University Malaysia, CDT 250, 98009 Miri, Sarawak, Malaysia

wastewater, owing to its technological importance in industries such as textile, battery manufacturing, and paint [4, 5]. They are harmful to humans, leading to a wide range of health problems, such as malfunctioning of the human central nervous system, immune system, excretory system, and cardiovascular system [6, 7]. Because of the non-biodegradability of heavy metals (i.e., lead) in the environment and their harmfulness to living organisms, their removal becomes crucial in protecting the ecosystem and human health [8].

Developing sustainable advanced processes is required for wastewater-containing heavy metal treatment to achieve environmental quality standards and protect water systems from potentially harmful contaminants. Adsorption is, by far, the most prominent alternative for removing Pb(II) from wastewater, owing to its most economical, efficient, and selective treatment method [9, 10]. For industrial wastewater treatment applications, a packed bed adsorption column is the most practical mode since it allows for large volume wastewater to be treated with a simple operation method [11–14]. Moreover, a packed bed adsorption column provides reliable information regarding the breakthrough curve (BTC) and mass transfer zone (MTZ), which is one of the critical aspects in evaluating the performance and feasibility of adsorbents for industrial applications [12, 15]. Surfing into literature found that adsorption processes in removing heavy metal ions were mainly conducted in batch experiments. Some similar authors have extended their investigation to a continuous lab-scaled packed bed column for breakthrough curve determination. Unfortunately, most researchers have yet to investigate the adsorbents that they developed for their performance behavior in the continuous packed bed column. This creates a gap between the batch and continuous analysis; therefore, there is a necessity in transitioning the data obtained from the batch study for the analysis in the continuous investigation.

The design and optimization of an industrial-sized packed bed column require a mathematical model that predicts the dynamic performance (i.e., breakthrough curve) is very important, thus significantly reducing the experimental efforts that are sometimes laborious and time-consuming. A simplified mathematical model is often employed to define the adsorption process in a continuous packed bed column. The establishment of such model serves as a foundation for developing a commercial process simulator, such as AspenTech Aspen Adsorption. The availability of such simulator made it possible to simulate the adsorption process by significantly reducing the burden of the manual handling of many equations and their numerical solutions. The use of such simulator is not limited to merely

solving some equations, but has expanded into the design and optimization of commercial processes [16].

Therefore, the objectives of this present paper are two-fold: First, to evaluate the adsorptive performance in an industrial-sized packed bed column for removing divalent lead ion, Pb(II) from aqueous solution by transitioning batch adsorption data to a continuous industrial-sized packed bed column through numerical computer simulation. The method here utilizes a simulation tool, Aspen Adsorption, to predict the breakthrough curve using minimum experimental data, and does not require obtaining model parameters from the experiment. The industrial-sized packed bed column specifications were taken from the real implemented adsorber column in the industry. Ten Langmuir-fitted adsorbents were selected for the evaluation of dynamic performance in an industrial-sized packed bed column for removing Pb(II). Their performances were measured in terms of saturation time, length of mass transfer zone, percentage removal, and breakthrough curve plot. Second, to compare their dynamic adsorption performances and formulate a simple analysis method to compare the adsorption performances based on the batch experimental information related to separation factor and total adsorbent mass, the simple analysis method was formulated based on the simulation results obtained in the first objective of this paper.

## 2 Theories and assumptions

### 2.1 Packed bed adsorption column simulation

The Aspen Adsorption simulation tool is used for the aqueous phase simulation study in removing Pb(II) using various adsorbents. Several assumptions are considered in order to model the packed bed adsorption column [17–19]:

1. The upward difference scheme 1 (UDS1) is used as a spatial domain discretization method, with 200 nodes within the confined axial column length.
2. The fluid flow behavior across the bed column length is assumed to be axially dispersed flow, with an isothermal condition along the bed.
3. The velocity variation along the bed is negligible due to constant fluid moment assumption.
4. Bed column porosity is uniform throughout the bed.
5. A lumped mass transfer model is considered with solid-film resistance. The lumped mass transfer consists of external film resistance and intraparticle resistance.
6. The adsorption equilibrium condition between the liquid and solid phases is described using the Langmuir isotherm.

## 2.2 Mathematical model framework

The formulation of the mathematical model for numerical simulation of the packed bed adsorption column is obtained through the differential mass balances for an elementary volume of Pb(II) in the fluid and solid phases. Considering a control volume with a height  $\Delta z$  and a cross-sectional area of the column  $A$ , a fluid stream containing Pb(II) to be adsorbed flows through the beds with void  $\epsilon$ . Then, the volume of solid  $V_s$  being the control volume is expressed in Eq. 1.

$$V_s = (1 - \epsilon)A\Delta z \tag{1}$$

Applying the mass balance of Pb(II) in the fluid phase of the inlet terms, outlet, and accumulation of the component in the control volume makes the following partial differential equations (PDEs) as depicted in Fig. 1 and expressed in Eq. 2.

$$(u_0\epsilon C)_z - (u_0\epsilon C)_{z+\Delta z} - \left(\epsilon E_z \frac{\partial C}{\partial z}\right)_z + \left(\epsilon E_z \frac{\partial C}{\partial z}\right)_{z+\Delta z} - \rho_s \Delta z \frac{\partial Q}{\partial t} = \epsilon \Delta z \frac{\partial C}{\partial t} \tag{2}$$

where  $E_z$  is the axial dispersion coefficient ( $m^2/s$ ),  $\rho_s$  is the bed column density ( $kg/m^3$ ),  $u_0$  is interstitial velocity ( $m/s$ ),  $z$  is the bed axial position ( $m$ ),  $t$  is the process time ( $s$ ),  $C$  is the aqueous phase concentration of Pb(II) ( $mg/L$ ), and  $Q$  is the solid-phase loading of Pb(II) ( $mg/g$ ). Applying the limit  $\Delta z \rightarrow 0$  and the definition of derivatives yield the overall mass balance as in Eq. 3.

$$u_0\epsilon \frac{\partial C}{\partial z} + \epsilon \frac{\partial C}{\partial t} + \rho_s \frac{\partial Q}{\partial t} = E_z \frac{\partial^2 C}{\partial z^2} \tag{3}$$

## 2.3 Adsorption rate using linear driving force (LDF) model

The kinetic mass transfer coefficient is adequately assumed to follow the LDF approximation as popularized by Glueckauf [20], in which the mass transfer driving force for Pb(II) is a linear function of the solid-phase loading [18]. The LDF model is often used in the analysis of the adsorption process due to its being mathematically simple without

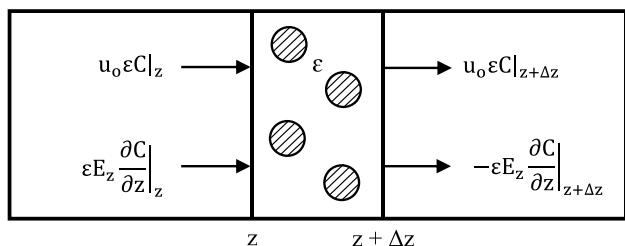


Fig. 1 Control volume for mass balance around adsorption packed bed column, as represented by Eq. 2

jeopardizing its accuracy [21]. The adsorption rate  $dQ/dt$ , for the LDF model can be written as shown in Eq. 4.

$$\frac{\partial Q}{\partial t} = k_{LDF}(Q^* - Q) \tag{4}$$

where  $k_{LDF}$  ( $1/s$ ) is the LDF mass transfer coefficient. In this work, the  $k_{LDF}$  is lumped by two mass transfer diffusion resistances: external film mass transfer diffusion,  $k_f$  ( $m/s$ ), and intraparticle surface mass transfer diffusion,  $k_s$  ( $m^2/s$ ). The correlations for calculating the  $k_{LDF}$ ,  $k_f$  and  $k_s$  are presented in Table 1.

## 2.4 Adsorption equilibrium isotherm

The non-linear Langmuir isotherm as expressed in Eq. 5 [22]

$$Q^* = \frac{Q_{max} K_L C^*}{1 + K_L C^*} \tag{5}$$

assumes that adsorption occurs on a homogenous surface in one layer (monolayer) without interaction between the adsorbed molecules. Langmuir isotherm is a two-parameter equation, consisting of  $Q_{max}$  and  $K_L$ . The  $Q_{max}$  ( $mg/g$ ) is the Langmuir maximum adsorption capacity, while  $K_L$  ( $L/mg$ ) is the Langmuir constant related to adsorption affinity. The variables  $Q^*$  ( $mg/g$ ) and  $C^*$  ( $mg/L$ ) are the solid-phase loading and liquid-phase concentration, respectively, both at the interphase. The Langmuir isotherm is one of the most frequently utilized isotherms in the literature, often providing good agreement with experimental data at very low concentration. This present work uses the isotherm parameters of  $Q_{max}$  and  $K_L$  obtained from the published works as stated in Section 3.1.

## 2.5 Numerical method

The Aspen Adsorption is used to solve the governing sets of partial differential equations (PDEs), ordinary differential equations (ODEs), and algebraic equations of the packed bed adsorption column model. Initially, the model equations of Eqs. 3–5 are spatially discretized into 200 nodes in the axial direction using the finite difference scheme, which is UDS1, as mentioned in Section 2.1, which turns the PDEs into sets of ODEs and algebraic equations. The first- and second-order differential terms of UDS1 for converting the PDEs into DAEs are expressed in Eq. 6 and Eq. 7 [18].

$$\frac{\partial \Gamma_i}{\partial z} = \frac{\Gamma_i - \Gamma_{i-1}}{\Delta z} \tag{6}$$

$$\frac{\partial^2 \Gamma_i}{\partial z^2} = \frac{\Gamma_{i+1} - 2\Gamma_i + \Gamma_{i-1}}{\Delta z^2} \tag{7}$$

**Table 1** Correlations used for estimating unknown model parameters

Model parameters	Condition	Formulation	Equation number
<i>External film mass transfer diffusion, <math>k_f</math> (m/s)</i>			
Ohashi correlation [23]	$0.001 < \text{Re} < 5.8$	$\text{Sh} = 2.0 + 1.58\text{Re}^{0.4}\text{Sc}^{\frac{1}{3}}$	Equation 8
	$5.8 < \text{Re} < 500$	$\text{Sh} = 2.0 + 1.21\text{Re}^{0.5}\text{Sc}^{\frac{1}{3}}$	Equation 9
<i>Intraparticle surface mass transfer diffusion, <math>k_s</math> (<math>\text{m}^2/\text{s}</math>)</i>			
Heese & Worch correlation [24]	-	$k_s = 8.6 \times 10^{-5} r_p \sqrt{\frac{D_p C_0}{Q_0}}$	Equation 10
<i>LDF mass transfer coefficient, <math>k_{LDF}</math> (1/s)</i>			
Approximation by Glueckauf [20]	-	$\frac{1}{k_{LDF}} = \frac{r_p}{3(1-\epsilon)k_f} + \frac{r_p^2}{15k_s}$	Equation 11
<i>Axial dispersion coefficient, <math>E_z</math> (<math>\text{m}^2/\text{s}</math>)</i>			
Wakao and Funazkri correlation [25, 26]	-	$E_z = 2\text{ur}_p \left[ \frac{20}{\text{ReSc}} + \frac{1}{2} \right]$	Equation 12

where  $\Gamma$  and  $i$  represent the dependent variable and position, respectively. Then, the resulting system of DAEs is solved simultaneously, with respect to both space and time. An implicit Euler method is used as an integrator for solving the ODEs, and the concentration profile of a packed bed adsorption column is obtained as a function of axial position and time (breakthrough curve profile).

## 2.6 Correlations used for estimation of unknown transport properties

The use of available correlations for estimating unknown model parameters, which is the transport properties, such as mass transfer coefficient and axial dispersion coefficient, is important for solving the balance equations and predict the dynamics of a packed bed adsorption column. Thus, few correlations have been selected to range the operating conditions in this study. Equations 8 to 12 represent the correlations used for estimating the unknown transport properties in this simulation work, as listed in Table 1.

## 2.7 Simulation procedure

The simulation starts with importing the feed component (in this case is  $\text{Pb}(\text{NO}_3)_2$ ) from Aspen Properties database. Then, the calculation proceeds with the required input parameters fed into the main simulation tool, Aspen Adsorption, such as the physical properties of adsorbents, operational feed conditions, packed bed column properties, transport properties, and isotherm parameters. The output generated is in the form of a breakthrough curve, calculated through numerical iterations of the set of governing equations, as described in Section 2.5, and the obtained data are analyzed to produce meaningful results. Figure 2 shows the simulation procedure used in this work.

## 3 Materials and methodology

### 3.1 Case studies

This study is based on the data extracted from several published papers that are used as case studies in this current work. The dynamic adsorption simulations are conducted using Aspen Adsorption. The list of selected published papers is presented in Table 2. Each adsorbent is assigned with a case number to simplify the use of each adsorbent in the text.

### 3.2 Extraction of required data for simulation

The required data for the simulation on the adsorbent properties and adsorption isotherm are presented in Table 3. This present work requires the determination of adsorption isotherm parameters and several adsorbent physical properties before the prediction of the breakthrough curves using the proposed method in this paper.

Most of the data in Table 3 will be generally available from the respective authors, since the adsorbent is characterized and isotherm should have been determined. Otherwise, some experiments should be carried out before applying the method proposed in this present work in order to predict the behavior of the packed bed column. To initialize the simulation, a bed voidage,  $\epsilon$ , is required as described in Eq. 3. Bed voidage is a fraction of the total volume, which is free spaces available for the fluid flow. In a packed bed column, the bed voidage for solid materials is often in the range of 0.35–0.45 for a larger bed column diameter-to-particle diameter,  $D/d_p$  ratio [37–39]. Therefore, a median value of 0.4 is taken as the bed voidage for all the ten adsorbents used in this study.

**Fig. 2** Simulation procedure for generating breakthrough curves

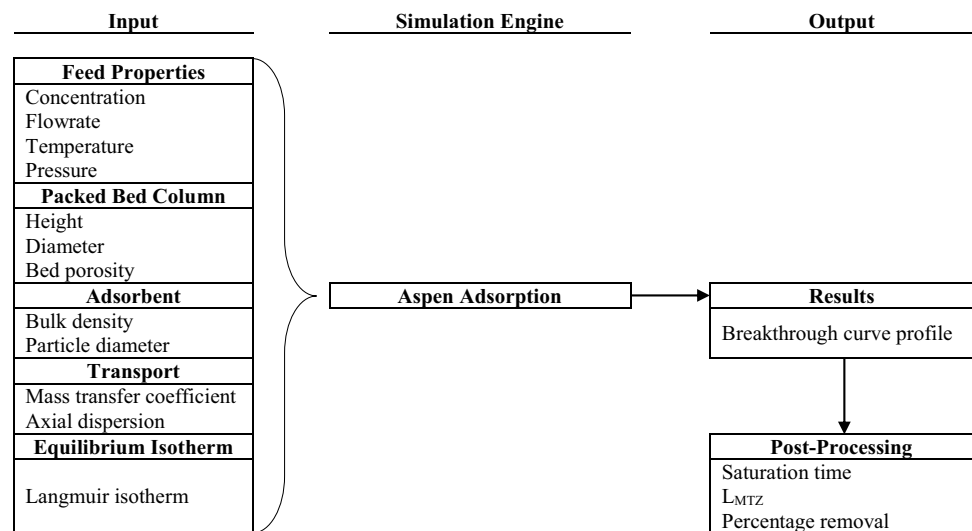


**Table 2** Ten selected published papers for the evaluation of Pb(II) removal by various adsorbents

Title of research paper(s)	Adsorbent	Case number	Reference
Removal of lead in water using activated carbon prepared from <i>Acacia catechu</i>	<i>Acacia catechu</i> AC	1	Lakshmikandhan and Ramadevi (2019) [27]
Adsorption of Pb(II) from aqueous solutions using activated carbon developed from apricot stone	Apricot stone AC	2	Mouni et al. (2011) [28]
Removal of Pb(II) by adsorption onto Chinese walnut shell-activated carbon	Chinese walnut shell AC	3	Yi et al. (2015) [29]
Removal of lead(II) by adsorption using treated granular-activated carbon: batch and column studies	Coconut shell AC	4	Goel et al. (2005) [30]
Adsorption of Cd(II) and Pb(II) ions from aqueous solutions using mesoporous-activated carbon adsorbent: equilibrium, kinetics, and characterisation studies	Commercial mesoporous AC	5	Asuquo et al. (2017) [31]
Adsorption of Pb(II) ions from aqueous solutions by date bead carbon activated with ZnCl <sub>2</sub>	Date bead AC	6	Danish et al. (2011) [32]
Adsorption of lead(II) from aqueous solution by activated carbon prepared from <i>Eichhornia</i>	<i>Eichhornia</i> AC	7	Shekinah et al. (2002) [33]
Kinetic and equilibrium modeling of liquid-phase adsorption of lead and lead chelates on activated carbons	Saw dust AC	8	Krishnan, Sheela and Anirudhan (2003) [34]
Adsorption study of lead(II) onto xanthated date palm trunk: kinetics, isotherm and mechanism	Xanthated date palm kernel trunk	9	Yadav, Singh and Sinha (2013) [35]
Removal of lead(II) from waste water on zeolite-NaX	Zeolite NaX	10	Pandey, Sharma and Sambhi (2015) [36]

### 3.3 Specifications of industrial-sized packed bed column

The dynamic adsorption performances of Pb(II) removal in a packed bed column for ten adsorbents were tested individually on an industrial-sized column. The industrial-sized packed bed column specifications for arsenic removal are taken from an actual packed bed column plant size as a case study to initialize the simulation. The design specifications

of the industrial-sized packed bed column are summarized in Table 4 [40]. As a comparison, several specifications of other typical industrial adsorbents can be found in Table S1 in the Supplementary Materials.

The concentration of Pb(II) in industrial effluent differs from one source point to another. Therefore, the concentration of Pb(II) used for this simulation work is taken from a real textile industrial effluent as investigated by [41]. The Pb(II) concentration is taken as 0.1 mg/L.

**Table 3** Required data extracted from the published papers that are used in the simulation of Pb(II) removal by ten adsorbents

Descriptions	Case									
	1	2	3	4	5	6	7	8	9	10
Adsorbent bulk density, $\rho_s$ (kg/m <sup>3</sup> )	766	810	575	500	690	1196	120	612	1,120	600
Adsorbent particle diameter, $d_p$ ( $\mu\text{m}$ )	575	188	1,023	1,611	425	125	153	96.0	75.0	1500
<i>Isotherm parameters</i>										
$Q_{\text{max}}$ or $\text{IP}_1$ (mg/g)	80.0	21.4	82.0	21.9	20.3	76.9	16.6	149	53.5	14.2
$K_L$ or $\text{IP}_2$ (L/mg)	0.256	5.69	0.151	3.51	0.110	0.209	1.00	0.00840	0.175	0.0976

The source papers are listed in Table 2

**Table 4** Some basic design specifications of the industrial-sized packed bed column

Specification	Value
Feed flowrate, $Q$ (m <sup>3</sup> /s)	$6.31 \times 10^{-4}$
Bed column height, $H$ (m)	0.9730
Bed column diameter, $D$ (m)	0.6096

Taken from [40]

### 3.4 Dynamic adsorption performance analysis

The results from the converged simulation are presented in data tables and graphical presentations. Several indexes are used to describe the dynamic adsorption performance in a packed bed column, including breakthrough time ( $t_b$ ), saturation time ( $t_s$ ), length of mass transfer zone ( $L_{\text{MTZ}}$ ), and percentage removal ( $R\%$ ). The breakthrough time,  $t_b$  (day), is taken at a time when the  $C/C_0$  reached 0.05, while the saturation time,  $t_s$  (day), is taken at a time when the  $C/C_0$  reached 0.95. The  $L_{\text{MTZ}}$  (m) is calculated following Eq. 13.

$$L_{\text{MTZ}} = H \left( 1 - \frac{t_b}{t_s} \right) \quad (13)$$

where  $H$  is the bed column height (m). The Pb(II) percentage removal ( $R\%$ ) is determined through the column maximum capacity calculation. At a given inlet adsorbate solution flowrate and concentration, the total amount of Pb(II) adsorbed in the column,  $Q_{\text{total}}$  (kmol), can be calculated from the area under the breakthrough curve as expressed in Eq. 14.

$$Q_{\text{total}} = F \int_{t=0}^{t=t_s} \left( 1 - \frac{C_t}{C_0} \right) dt \quad (14)$$

where  $F$  is the inlet flowrate (m<sup>3</sup>/s) and  $C_t/C_0$  is the normalized outlet concentration at time  $t$ . The amount of Pb(II) entering the bed column,  $M_{\text{total}}$  (kmol), is determined using Eq. 15.

$$M_{\text{total}} = FC_0 t_s \quad (15)$$

where  $C_0$  is the inlet concentration (kmol/m<sup>3</sup>). Finally, the percentage removal of Pb(II) ( $R\%$ ) is calculated by applying Eq. 16.

$$R\% = \frac{Q_{\text{total}}}{M_{\text{total}}} \times 100\% \quad (16)$$

## 4 Results and discussion

In the present work, the prediction of the dynamic performance of a packed bed adsorption column using numerical simulation with minimum experimental data needed and other unknown model parameters calculated using well-established correlations is key to this paper. Many batch adsorption systems can be extended to a continuous packed bed adsorption column system. The validity of the robustness of the LDF model employed in this present work has been proven by several investigators that model the aqueous phase breakthrough curves for adsorption in a packed bed column [17, 42–44], in which the explanation of the verification methods was presented in Table S2 in the Supplementary Materials.

### 4.1 Analysis of the dynamic performance of various adsorbents for Pb(II) removal

The LDF mathematical model of the packed bed adsorption column is solved numerically using a simulation tool, Aspen Adsorption, following the assumptions considered in Section 2.1. The converged simulation results are presented in data tables and graphical presentations. The performance of the packed bed adsorption column is evaluated by analyzing the saturation time ( $t_s$ ), length of mass transfer zone ( $L_{\text{MTZ}}$ ), and percentage removal ( $R\%$ ), and breakthrough curve for all ten adsorbents is presented in Table 5.

The shape and gradient of the breakthrough curves (BTC) were determined and controlled by the mass

transfer diffusion of Pb(II) from the bulk solution to the adsorbent's surfaces. Steeper BTC is formed when the mass transfer resistance is small, and vice versa. Negligible mass transfer resistance forms the ideal step-size function BTC. However, the real BTC always deviates from the ideal BTC due to mass transfer resistance, as shown in Table 5. From the BTC, important information regarding the operation time of the bed column can be obtained. Breakthrough time and saturation time are often extracted from the breakthrough curve as indicators to determine the dynamic performance of an adsorbent in a packed bed column. Here, the saturation time was taken as an indicator of the operational lifespan of the packed bed column before media regeneration or replacement. Among the adsorbents studied here, apricot stone AC showed the longest saturation time in an industrial-sized packed bed column for removing Pb(II), with a saturation time of 203 days, while the shortest saturation time belongs to saw dust AC, with a saturation time of 3.10 days. Apricot stone AC, the organic adsorbent, seems superior in removing Pb(II) compared to inorganic adsorbents, such as zeolite NaX. When comparing among the organic adsorbents, some bio-activated carbons perform better in an industrial-sized packed bed column than commercial-activated carbon. This could bring alternatives of cheaper adsorbents for removing Pb(II) from an aqueous solution. Thus, the prospect of finding economic and environmental-friendly adsorbents could potentially become a reality to be implemented for industrial application for removing Pb(II)-containing wastewater.

Another index measure in analyzing the dynamic performance of a packed bed column is the mass transfer zone. The mass transfer zone develops from the inlet side in the column and progressively transverses towards the outlet side. In defining the dynamic performance of a packed bed column, mass transfer zone is often expressed

as the  $L_{MTZ}$ . It characterizes the wavefront of the packed bed column, and an ideal wavefront has zero  $L_{MTZ}$  because it forms a step-size function due to the absence of mass transfer resistance. Thus, shorter  $L_{MTZ}$  suggests an efficient utilization of the adsorbent bed. The  $L_{MTZ}$  can be graphically observed from the breakthrough curve (BTC), as depicted in Fig. 3, in which a steeper BTC has shorter  $L_{MTZ}$ , and a broader BTC has longer  $L_{MTZ}$ . Table 5 shows that the apricot stone AC has the shortest  $L_{MTZ}$  and, correspondingly, the steepest BTC, whereas, the Chinese walnut shell AC has the longest  $L_{MTZ}$ ; thus, has the broadest BTC. Also, in Table 5, it is demonstrated that the apricot stone AC has the highest percentage removal,  $R\%$  (95.6%), and the Chinese walnut shell AC has the lowest percentage removal,  $R\%$  (56.8%). It is worth pointing out that the  $L_{MTZ}$  and  $R\%$  can be described as being inversely proportional to each other; the lower the  $L_{MTZ}$ , the higher the  $R\%$ . This is due to the fact that a shorter  $L_{MTZ}$  represents only a small portion of the adsorbent zone that is not utilized for the adsorption process [45, 46].

## 4.2 Discussion on isotherm data using Langmuir equation

The respective Langmuir isotherm parameters for all ten adsorbents studied here were used to re-plot the adsorption isotherm graph at the desired range of inlet Pb(II) concentration,  $C_0$ . This is to understand the isotherm behavior of each adsorbent to support the simulation results in Section 4.1.

The Langmuir separation factor,  $R_L$ , is one of the essential characteristics of a Langmuir isotherm, which can be expressed by Eq. 17 [47].

$$R_L = \frac{1}{1 + K_L C_0} \quad (17)$$

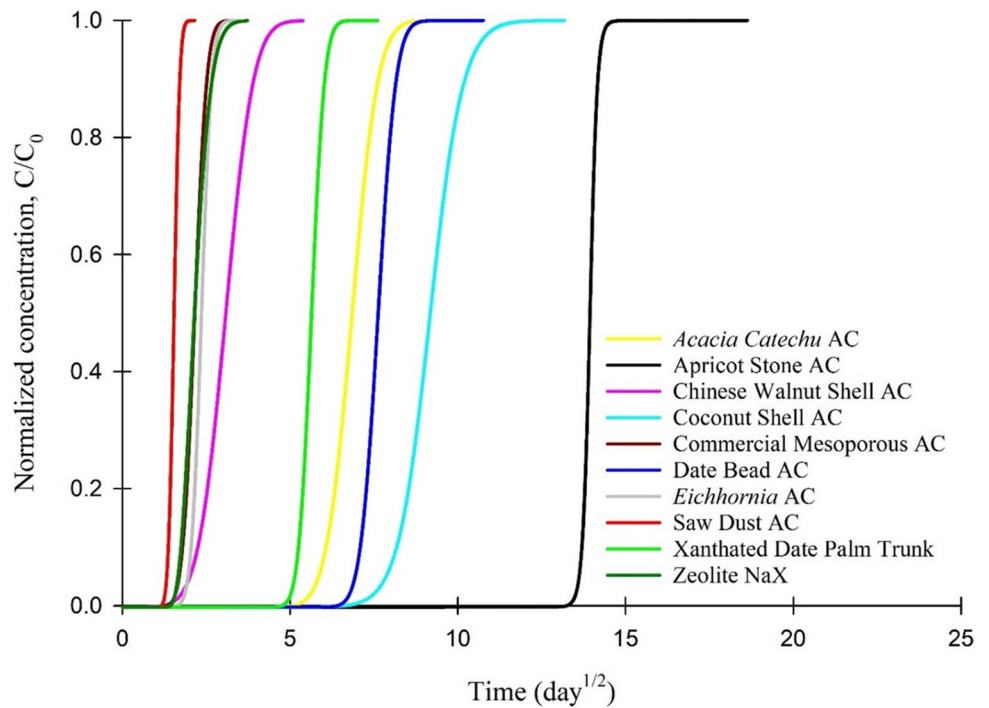
According to [47], the parameter  $R_L$  indicates favorable isotherm type if the value is within  $0 < R_L < 1$ , and a very favorable isotherm is indicated by a value closer to zero. Linear isotherm type has the  $R_L = 1$ . Referring to Fig. 4 and Table 6, the adsorbents having  $R_L > 0.9$  seem to have a linear curve, whereas two adsorbents, which are the apricot stone AC (red line) and the coconut shell AC (lime line), have convex curves. This indicated favorable adsorption by the apricot stone AC and the coconut shell AC at Pb(II) concentration of 0.1 mg/L. Note that the favorability of the adsorption process varies with concentration. Depending on the concentration, an adsorbent may have a favorable isotherm at one concentration, whereas the isotherm might be linear at a different concentration.

The Langmuir separation factor,  $R_L$ , always corresponds to the solid-phase loading fraction at inlet concentration

**Table 5** Ranking of industrial-sized packed bed column performance of ten adsorbents for removing heavy metal lead ion arranged in descending order w.r.t. the saturation time,  $t_s$  ( $F=631$  mL/s,  $C_0=0.1$  mg/L,  $H_b=0.973$  m,  $D=0.6096$  m)

Adsorbents	$t_s$ (days)	$L_{MTZ}$ (m)	$R$ (%)
Apricot stone AC	203	0.0857	95.6
Coconut shell AC	111	0.435	76.5
Date bead AC	69.2	0.299	84.2
<i>Acacia catechu</i> AC	61.7	0.436	76.6
Xanthated date palm trunk	37.8	0.295	87.5
Chinese walnut shell AC	17.3	0.748	56.8
Zeolite NaX	8.07	0.645	60.5
<i>Eichhornia</i> AC	7.49	0.486	73.7
Commercial mesoporous AC	6.88	0.573	68.5
Saw dust AC	3.10	0.428	77.0

**Fig. 3** The breakthrough curves of ten adsorbents for removing Pb(II) in an industrial-scaled packed bed column



(in this case is 0.1 mg/L),  $Q_0/Q_{max}$ , but not always to the total amount adsorbed by the adsorbent mass,  $m_{total}$ . This is because the calculation of  $m_{total}$  includes the value of bulk solid density, which varies from one adsorbent to another. The  $m_{total}$  implies a capacity or amount of the adsorbate (Pb(II)) that a specific amount of adsorbent can hold.

**4.2.1 Relation between  $R_L$ ,  $Q_0/Q_{max}$  and  $t_s$**

Looking at Fig. 4, and information on  $R_L$  and  $Q_0/Q_{max}$  from Table 6, the ranking of dynamic performance of each adsorbent should be as follows:  $2 > 4 > 7 > 1 > 6 > 9 > 3 > 5 > 10 > 8$ . However, the actual ranking in terms of the saturation

**Fig. 4** Langmuir adsorption isotherm plot for ten adsorbents at liquid concentration ranges from 0.0–0.5 mg/L. Note that the present study works on 0.1 mg/L inlet concentration

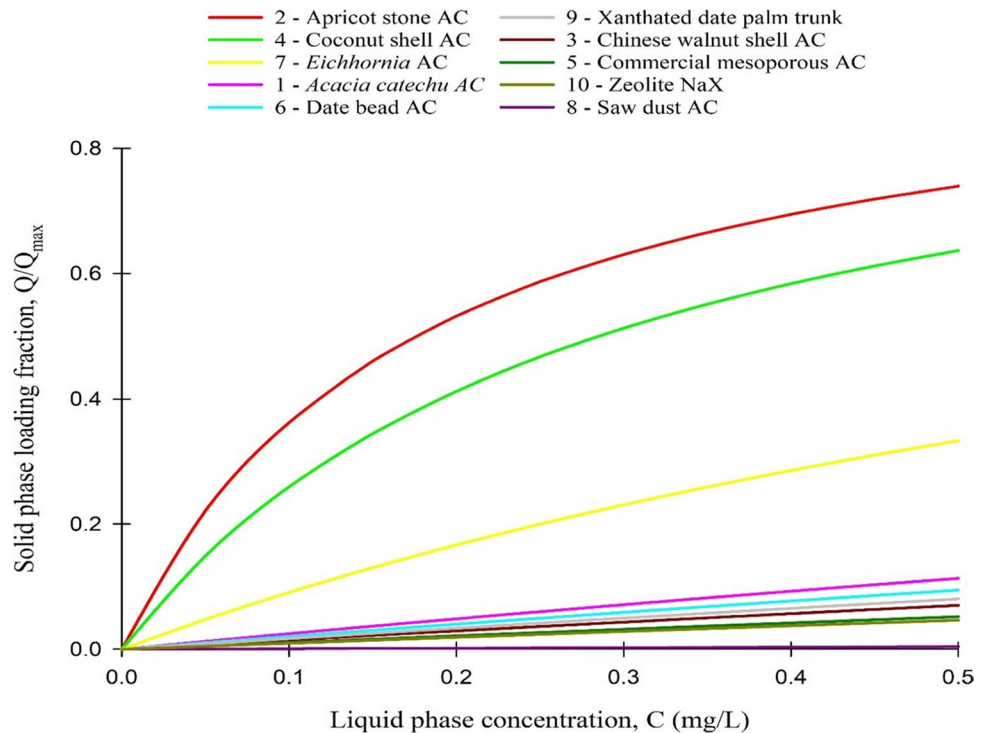




**Table 6** The Langmuir isotherm characteristics of ten adsorbents, arranged in descending order w.r.t. the total amount adsorbed by the adsorbent mass,  $m_{\text{total}}$ 

Adsorbent	Total amount adsorbed by the adsorbent mass, $m_{\text{total}}$ (kg)	Solid-phase loading fraction at 0.1 mg/L, $Q/Q_{\text{max}}$	Langmuir separation factor at 0.1 mg/L, $R_L$
Apricot stone AC	33.4	0.363	0.637
Coconut shell AC	14.8	0.260	0.740
Date bead AC	2.78	0.0205	0.980
Xanthated date palm trunk	2.19	0.0172	0.983
<i>Acacia catechu</i> AC	2.17	0.0249	0.975
<i>Eichhornia</i> AC	1.24	0.0909	0.909
Chinese walnut shell AC	0.972	0.0149	0.985
Commercial mesoporous AC	0.853	0.0109	0.989
Zeolite NaX	0.659	0.00967	0.990
Saw dust AC	0.0595	0.000841	0.999

time from the simulation results is as follows:  $2 > 4 > 6 > 1 > 9 > 3 > 10 > 7 > 5 > 8$ . In general, the lower the  $R_L$ , the longer the adsorbent reaches the breakthrough and saturation points, due to favorable adsorption at lower  $R_L$  [48]. Nevertheless, inconsistency was observed between the  $R_L$  trend and saturation time. The fluctuations of  $R_L$  towards the saturation time ranking were due to different adsorbent physical properties of each, such as bulk solid density that may affect the Reynolds number of the fluid flow inside the bed column, thereby affecting the amount adsorbed from the liquid to the solid phases. Nonetheless, the parameter  $R_L$  is suitable to be used only as a preliminary relative comparison of adsorbent performance indicator from the fundamental information related to isotherm, without considering the adsorbent properties.

From Table 5 in Section 4.1, apricot stone AC shows the longest saturation time, and saw dust AC shows the shortest saturation time. When comparing the physical properties, such as the BET surface area of each adsorbent, no relationship was observed that concurs with the ranking of the  $t_s$  (see Table S3 in the Supplementary Materials). However, the outcome concurs with the values of  $R_L$ , as stated in Table 6, in which the  $R_L$  for apricot stone AC is close to zero, while saw dust AC reported the highest  $R_L$  among the adsorbents studied here, with a value of 0.9992. Therefore, if one wishes to compare two or more adsorbents to be used in a packed bed column, the information on  $R_L$  obtained from batch adsorption analysis can be used to make a preliminary guess about which adsorbent performs better in a packed bed column, without taking into consideration of adsorbent bulk solid density.

#### 4.2.2 Relation between $m_{\text{total}}$ and $t_s$

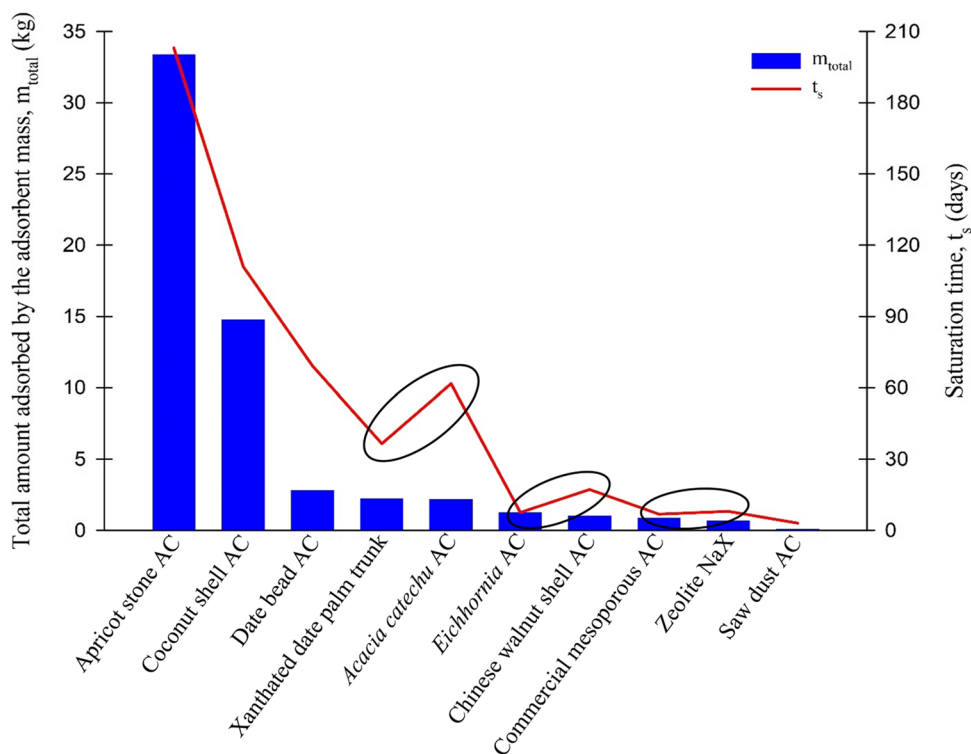
The operation time of an adsorbent in a packed bed column can be related to the total amount of adsorbate adsorbed

by the adsorbent mass,  $m_{\text{total}}$ . The  $m_{\text{total}}$  is a multiplication product between the total amounts of adsorbent mass in the column,  $m_{\text{ads}}$  (kg), and the solid-phase loading fraction,  $Q/Q_{\text{max}}$ . The higher the  $m_{\text{total}}$ , the longer the operational time (or saturation time) of the adsorbent in the packed bed column. Figure 5 shows the trend and relation between the  $m_{\text{total}}$  and saturation time,  $t_s$ , for ten adsorbents. The  $t_s$  obtained from the simulation results agree with the trend in the  $m_{\text{total}}$  of the adsorbents. However, some inconsistencies are observed, which showed fluctuations in the three pairs of adsorbents (indicated in the oval), as presented in Fig. 5. The most reasonable explanation for the inconsistencies is due to the dissimilarity in the adsorbent particle sizes of each adsorbent, as stated in Table 3. Since different adsorbent particle sizes cause different fluid flows across the adsorbent particles, thereby, affecting the mass transfer diffusion during the adsorption process, the reason for the inconsistency for the three pairs of adsorbents will be confirmed in the following subsection. As opposed to  $R_L$ , the parameter  $m_{\text{total}}$  is a more reliable means of comparing adsorbent performance for the packed bed column, since it incorporates both information related to isotherm and adsorbent properties of bulk solid density.

The plot of the total amount adsorbed by the adsorbent mass,  $m_{\text{total}}$ , versus the saturation time,  $t_s$ , obtained from the breakthrough curves modeling and the calculation from isotherm parameters and bulk solid density are compared in Fig. 6. The trend in Fig. 6 shows general agreement in the relationship between  $m_{\text{total}}$  and  $t_s$ , though more adsorbents need to be included in the list for better quantitative agreement. It can be presumed that the relationship between the  $m_{\text{total}}$  and  $t_s$  shows a positive linear relationship with each other.

Also, as shown in the ranking of adsorbents in Fig. 6, the biomass-activated adsorbents are the most promising, as they outperform the commercial organic and inorganic adsorbents in terms of their dynamic performance, which is

**Fig. 5** The total amount adsorbed by the adsorbent mass,  $m_{\text{total}}$  at inlet concentration of 0.1 mg/L and the corresponding saturation time of each adsorbent. The adsorbents were arranged in descending order w.r.t.  $m_{\text{total}}$



expressed as the saturation time. It is, however, important to consider not only the dynamic performance of the adsorbents when evaluating them in packed bed columns, but also the economic analysis of the adsorbents to determine whether the performance outweighs any potential drawbacks such as the cost, long-term stability, and difficulty of accessing and activating the raw materials.

### 4.3 Sensitivity analysis of the breakthrough curves

Sensitivity analysis was performed to observe the influence of uncertainties in the model parameters (i.e.,  $k_{\text{LDF}}$  and  $E_z$ ) on the dynamic performance of a packed bed column. It measures the impacts of fluctuations in the parameters on the outputs or performance of the system. Both the  $k_{\text{LDF}}$  and  $E_z$  influence the column performance by altering the degree of the effectiveness of the transference of Pb(II) from the liquid to the solid adsorbent phases. The sensitivity analysis conducted here serves to ascertain the degree to which inaccuracies in their assumed values could lead to severe prediction errors and to confirm the inconsistencies observed in Section 4.2.2.

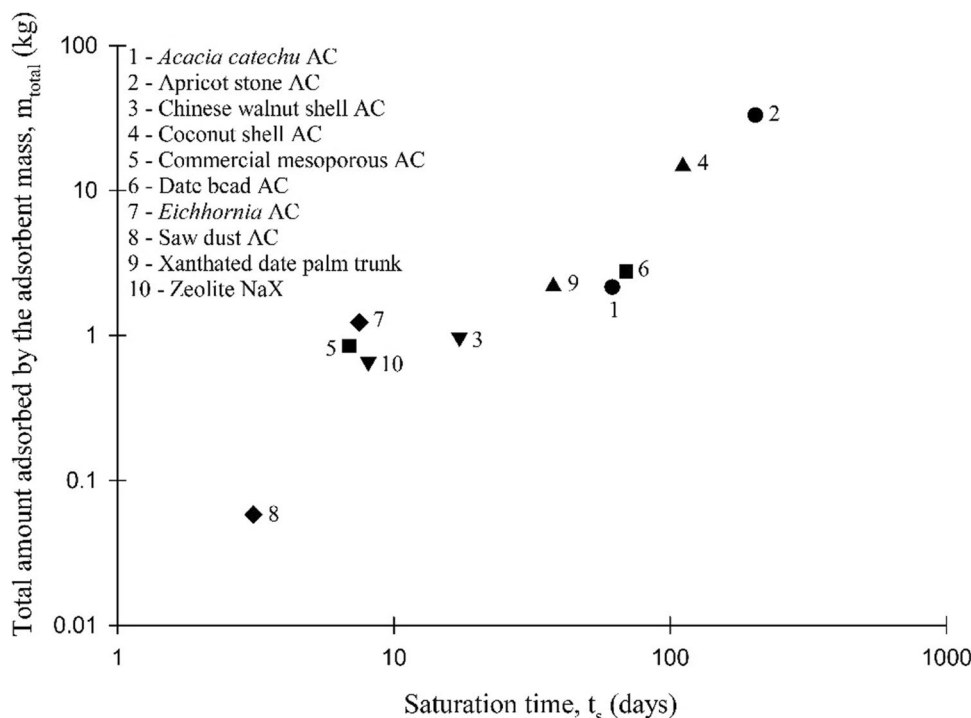
As the  $k_{\text{LDF}}$  is the inverse of the mass transfer resistance, higher  $k_{\text{LDF}}$  means lower resistance for the transference of Pb(II) molecules from the bulk solution to the adsorbent's surfaces, subsequently faster transference. Lower mass transfer resistance can be deduced from the BTC graph of having a steeper curve, which shifting the saturation time to the left, hence decreasing the saturation time. Conversely, higher  $E_z$  tends to flatten the

BTC, shifting the saturation time to the right, thus increasing the saturation time. This is probably due to turbulent occurrence as giving more effect when  $E_z$  increases.

The sensitivity analysis was conducted on three pairs of adsorbents (total of six adsorbents) that showed inconsistency in the saturation time with respect to  $m_{\text{total}}$ . The three pairs are (1) xanthated date palm trunk and *Acacia catechu* AC, (2) *Eichhornia* AC and Chinese walnut shell AC, and (3) commercial mesoporous AC and zeolite NaX. The parameter sensitivity analysis was expressed in terms of the relative change of research objective ( $t_s$ ) versus the relative change of the variables under investigation ( $k_{\text{LDF}}$  and  $E_z$ ). The results of  $\Delta t_s/t_s$  in Table 7 indicate that  $k_{\text{LDF}}$  influences the breakthrough curves more than  $E_z$ . On the other hand, a significant deviation in  $E_z$  estimation ( $\pm 200\%$ ) does not significantly affect the overall breakthrough curve and the saturation time. Thus, the following paragraph will focus on the sensitivity of  $k_{\text{LDF}}$  on the breakthrough curve, especially the saturation time, to support the inconsistency of the observed trend in Section 4.2.2.

Supposedly, xanthated date palm trunk should have a relatively longer saturation time than *Acacia catechu* AC because its  $m_{\text{total}}$  value is higher (2.1881 kg > 2.1692 kg). However, simulation results showed that *Acacia catechu* AC has a longer saturation time than xanthated date palm trunk. The inconsistency in the ranking of saturation time between xanthated date palm trunk and *Acacia catechu* AC can be well-compensated by the LDF mass transfer coefficient,  $k_{\text{LDF}}$  estimated values. The values of  $m_{\text{total}}$  of both

**Fig. 6**  $m_{total}$  versus  $t_s$  for Pb(II) removal on ten adsorbents



adsorbents were very close to each other. Consequently, their saturation time is also close to each other, as presented in Table 5. A change in the  $k_{LDF}$  value can change the saturation time because it affects the gradient of the breakthrough

curve, hence the  $L_{MTZ}$ . Referring to the  $L_{MTZ}$  parameter of both xanthated date palm trunk and *Acacia catechu* AC from Table 5, *Acacia catechu* AC showed higher  $L_{MTZ}$  than the xanthated date palm trunk. This means that the breakthrough

**Table 7** The details of sensitivity analysis of  $k_{LDF}$  and  $E_z$  on three pairs of adsorbents (six adsorbents) that show anomaly in the ranking of saturation time

Sensitivity parameters		LDF mass transfer coefficient, $k_{LDF}$ (1/s)				Axial dispersion coefficient, $E_z$ (m <sup>2</sup> /s)			
		-200%	-20%	+20%	+200%	-200%	-20%	+20%	+200%
Xanthated date palm trunk	$t_s$	38.5	38.0	37.7	37.4	37.8	37.8	37.8	37.8
	$\Delta t_s/t_s$ (%)	1.88	0.494	-0.340	-1.05	-0.0262	-0.0106	0.0106	0.0525
	$L_{MTZ}$ (m)	0.324	0.302	0.290	0.279	0.295	0.295	0.295	0.296
<i>Acacia catechu</i> AC	$t_s$	66.6	63.0	60.8	58.7	61.7	61.7	61.7	61.8
	$\Delta t_s/t_s$ (%)	7.28	2.10	-1.55	-5.14	-0.0991	-0.0394	0.0398	0.197
	$L_{MTZ}$ (m)	0.532	0.464	0.415	0.366	0.435	0.435	0.437	0.439
<i>Eichhornia</i> AC	$t_s$	8.36	7.69	7.32	6.94	7.49	7.49	7.49	7.50
	$\Delta t_s/t_s$ (%)	10.3	2.51	-2.34	-8.03	-0.0186	-0.00620	0.00710	0.0374
	$L_{MTZ}$ (m)	0.616	0.521	0.459	0.386	0.489	0.489	0.489	0.490
Chinese walnut shell AC	$t_s$	20.5	18.1	16.6	15.1	17.2	17.2	17.3	17.3
	$\Delta t_s/t_s$ (%)	15.8	4.95	-3.92	-14.1	-0.0500	-0.0200	0.0202	0.101
	$L_{MTZ}$ (m)	0.871	0.789	0.714	0.623	0.747	0.748	0.748	0.749
Commercial mesoporous AC	$t_s$	7.73	7.12	6.71	6.33	6.88	6.88	6.88	6.89
	$\Delta t_s/t_s$ (%)	11.0	3.32	-2.54	-8.77	-0.0442	-0.0175	0.0182	0.0889
	$L_{MTZ}$ (m)	0.694	0.610	0.543	0.471	0.572	0.573	0.573	0.574
Zeolite NaX	$t_s$	9.96	8.59	7.70	6.86	8.07	8.07	8.08	8.08
	$\Delta t_s/t_s$ (%)	18.9	6.06	-4.85	-17.7	-0.0471	-0.0184	0.0195	0.0947
	$L_{MTZ}$ (m)	0.820	0.703	0.597	0.469	0.644	0.645	0.645	0.647

\*Negative values of  $\Delta t_s/t_s$  indicate that the change of  $k_{LDF}$  and  $E_z$  from the original values steepened the breakthrough curve (lower  $L_{MTZ}$ )

curve of *Acacia catechu* AC was broader and spread out. Broadened and spread out breakthrough curve lengthen the saturation time, thus making *Acacia catechu* AC having a higher saturation time than xanthated date palm trunk. On the other hand, the breakthrough curve of xanthated date palm trunk was steeper, hence, shortening the saturation time, progressively towards its idealized breakthrough curve (imaginary step-size function).

The inconsistency in  $k_{LDF}$  between the pairs of adsorbents was due to different adsorbent particle sizes, which may affect the Reynolds number of the fluid flow inside the bed column, thus affecting the amount adsorbed from the liquid to solid phases. This is because the estimation of  $k_{LDF}$  involves the parameter of adsorbent particle size, as shown in the correlation in Table 1. Looking at the dissimilarities of adsorbent particle size of the xanthated date palm trunk and *Acacia catechu* AC from Table 3, the xanthated date palm trunk has a particle size of 75  $\mu\text{m}$ . In comparison, the *Acacia catechu* AC has a particle size of 575  $\mu\text{m}$ . The difference between both particle sizes is 500  $\mu\text{m}$ , or in a ratio of over 7.6. A large variance in the adsorbent particle size between these two could lead to a significant deviation in the  $k_{LDF}$  estimation value. Therefore, the sensitivity analysis tested on the  $k_{LDF}$  estimated value took a range of  $\pm 200\%$ , to establish the foundation on the degree of  $k_{LDF}$  deviation on the saturation time. Note that the sensitivity results in Table 7 may not reach the trend of  $m_{\text{total}}$  with  $t_s$  (Fig. 5), due to the limited range of sensitivity analysis study. Nevertheless, it serves as a basis for explaining the inconsistency that arose (see Table S4 in the Supplementary Materials). The same reason was applied for the pair of *Eichhornia* AC and Chinese walnut shell AC and commercial mesoporous AC and zeolite NaX.

## 5 Conclusion

The present work was confined to a systematic evaluation of the performance of an adsorbent in an industrial-scaled packed bed column for removing lead heavy metal ion, by means of computer simulation. The dynamic performance of ten adsorbents in an industrial-sized packed bed column for lead ion removal was analyzed through graphical and tabulated data analysis. The dynamic performances of an industrial-sized packed bed column were analyzed using the information of saturation time ( $t_s$ ), length of mass transfer zone ( $L_{MTZ}$ ), and percentage removal ( $R\%$ ).

The relationship between  $L_{MTZ}$  and  $R\%$  was found to be inversely proportional to each other. The parameter Langmuir separation factor ( $R_L$ ) was related to the favorability of the adsorption process. The fluctuations of  $R_L$  with the trend of  $t_s$  were due to dissimilarity of adsorbent bulk solid

density of each adsorbent. Meanwhile, the parameter  $m_{\text{total}}$  was related to the amount of adsorbate that the total mass adsorbent can hold. The inconsistency of several adsorbents with the trend of  $t_s$  was related to the dissimilarity of the adsorbent particle sizes of each adsorbent. The sensitivity analysis on the  $k_{LDF}$  confirmed the inconsistency of  $m_{\text{total}}$  trend with  $t_s$ . The preliminary relative performance indicator of an adsorbent in a packed bed column can be well-represented by the  $m_{\text{total}}$  value of each adsorbent. Nonetheless, in case of availability of only a fundamental information related to adsorption isotherm, the value of  $R_L$  can be used as a substitute to  $m_{\text{total}}$ , as a measure to the preliminary relative performance of an adsorbent.

To conclude, this study could give beneficial insights into how different adsorbents' performance differs when conducted in a continuous packed bed column, by measuring their respective  $R_L$  and  $m_{\text{total}}$ . This should serve as a stepping stone in comparing various adsorbents' performance operated in an industrial-packed bed column. Furthermore, by using the proposed method from this work, a review of breakthrough curves of many adsorbents in a packed bed column in removing specific pollutants can be accomplished through numerical simulation with minimum experimental effort. This ultimately saves time and cost as the design of an industrial adsorption process requires the investigations of many parameters that are always related to high investment, and it can also take a significant period of time.

**Supplementary Information** The online version contains supplementary material available at <https://doi.org/10.1007/s13399-022-03379-z>.

**Author contribution** Mohd Hardiyanto Vai Bahrn: Conceptualization, formal analysis, investigation, writing-original draft preparation. Awang Bono: Supervision, conceptualization, formal analysis, review, and editing. Muhammad Abbas Ahmad Zaini: Supervision, review, and editing. Norasikin Othman: Supervision, review, and editing. Agus Saptoro: Supervision, review, and editing.

**Data availability** Not applicable.

## Declarations

**Ethics approval** Not applicable.

**Competing interests** The authors declare no competing interests.

## References

- Kelishadi R (2012) Environmental pollution: health effects and operational implications for pollutants removal. *J Environ Public Health* 2012:341637
- Mayur R (1979) Environmental problems of developing countries. *Ann Am Acad Pol Soc Sci* 444:89–101
- Muralikrishna IV, Manickam V (2017) *Environmental management: science and engineering for industry*, 1st edn. Elsevier, Oxford, United Kingdom

4. Renu M, Agarwal K (2017) Singh, Heavy metal removal from wastewater using various adsorbents: a review. *J Water Reuse Desalin* 7:387–419
5. U.S. Department of Health and Human Services, Toxicological profile for lead. (2007).
6. Assi M, Hezmee M, Haron A, Sabri M, Rajion M (2016) The detrimental effects of lead on human and animal health. *Vet World* 9:660–671. <https://doi.org/10.14202/vetworld.2016.660-671>
7. Bahrun MHV, Kamin Z, Anisuzzaman SM, Bono A (2021) Assessment of adsorbent for removing lead (Pb) ion in an industrial-scaled packed bed column. *J Eng Sci Technol* 16:1213–1231
8. Ahmadi M, Teymouri P, Setodeh A, Mortazavi MS, Asgari A (2011) Adsorption of Pb(II) from aqueous solution onto Lewatit FO36 nano resin: equilibrium and kinetic studies. *Environ Eng Manag J* 10:1579–1587
9. Fu F, Wang Q (2011) Removal of heavy metal ions from wastewaters: a review. *J Environ Manage* 92:407–418
10. Vardhan KH, Kumar PS, Panda RC (2019) A review on heavy metal pollution, toxicity and remedial measures: current trends and future perspectives. *J Mol Liq* 290:111197
11. Hanafy H, Sellaoui L, Thue PS, Lima EC, Dotto GL, Alharbi T, Belmabrouk H, Bonilla-Petriciolet A, Ben Lamine A (2019) Statistical physics modeling and interpretation of the adsorption of dye remazol black B on natural and carbonized biomasses. *J.Mol Liq* 299:112099
12. Hu A, Ren G, Che J, Guo Y, Ye J, Zhou S (2020) Phosphate recovery with granular acid-activated neutralized red mud: fixed-bed column performance and breakthrough curve modelling. *J Environ Sci* 90:78–86
13. Ye N, Cimetiere N, Heim V, Fauchon N, Feliers C, Wolbert D (2019) Upscaling fixed bed adsorption behaviors towards emerging micropollutants in treated natural waters with aging activated carbon: model development and validation. *Water Res* 148:30–40. <https://doi.org/10.1016/j.watres.2018.10.029>
14. Paixão RM, Reck IM, Gomes RG, Bergamasco R, Vieira MF, Vieira AMS (2018) Water decontamination containing nitrate using biosorption with *Moringa oleifera* in dynamic mode. *Environ Sci Pollut Res* 25:21544–21554
15. Kamin Z, Bono A, Bahrun MHV (2021) Applicability of linear driving force (LDF) mass transfer model for heavy metal biosorption in packed bed column. *Mater Today Proc* 42:186–190. <https://doi.org/10.1016/j.matpr.2020.11.343>
16. Bahrun MHV, Battak N, Tan W-H, Bono A (2022) Process simulation of steam stripping of bleached palm oil deodorization for removing free fatty acids using DWSIM. *J Phys Conf Ser* 2314:012016. <https://doi.org/10.1088/1742-6596/2314/1/012016>
17. Danish M, Ansari KB, Danish M, Khan NA, Aftab RA, Zaidi S, Khan MS, Al Mesfer MK, Qyyum MA, Nizami AS (2022) Developing convective–dispersive transport model to characterize fixed-bed adsorption of lead (II) over activated tea waste biosorbent. *Biomass Convers Biorefinery*. <https://doi.org/10.1007/s13399-021-02130-4>
18. AspenTech A (2001) reference guide. Aspen Technology Inc, United Kingdom
19. Marin P, Borba CE, Módenes AN, Espinoza-Quñones FR, De Oliveira SPD, Kroumov AD (2014) Determination of the mass transfer limiting step of dye adsorption onto commercial adsorbent by using mathematical models. *Environ Technol (United Kingdom)* 35:2356–2364. <https://doi.org/10.1080/09593330.2014.904445>
20. Glueckauf E (1955) Theory of chromatography. Part 10: formulae for diffusion into spheres and their application to chromatography. *Trans Faraday Soc* 51:1540–1551. <https://doi.org/10.1039/TF9555101540>
21. Knox J, Ebner PAD, Levan MD, Coker RF, Ritter JA (2016) Limitations of breakthrough curve analysis in fixed-bed adsorption. *Ind Eng Chem Res* 55:4734–4748
22. Tan W-H, Bahrun MHV, Surugau N, Bono A (2020) Evaluation of adsorption dynamic retention of copper ion in porous agricultural soil. *Trans. Sci Technol* 7:90–100
23. Ohashi H, Sugawara T, Kikuchi K, Konno H (1981) Correlation of liquid-side mass transfer coefficient for single particles and fixed beds. *J Chem Eng Japan* 14:433–438
24. Sperlich A, Schimmelpfennig S, Baumgarten B, Genz A, Amy G, Worch E, Jekel M (2008) Predicting anion breakthrough in granular ferric hydroxide (GFH) adsorption filters. *Water Res* 42:2073–2082. <https://doi.org/10.1016/j.watres.2007.12.019>
25. Wakao N, Funazkri T (1978) Effect of fluid dispersion coefficients on particle-to-fluid mass transfer coefficients in packed beds: correlation of sherwood numbers. *Chem Eng Sci* 33:1375–1384
26. Bono A (1989) Sorptive separation of simple water soluble organics. University of Surrey.
27. Lakshmikanthan K, Ramadevi A (2019) Removal of lead in water using activated carbon prepared from *Acacia catechu*. *Water SA* 45:374–382
28. Mouni L, Merabet D, Bouzaza A, Belkhir L (2011) Adsorption of Pb(II) from aqueous solutions using activated carbon developed from apricot stone. *Desalination* 276:148–153
29. Yi ZJ, Yao J, Kuang YF, Chen HL, Wang F, Yuan ZM (2015) Removal of Pb(II) by adsorption onto Chinese walnut shell activated carbon. *Water Sci Technol* 72:983–989
30. Goel J, Kadirvelu K, Rajagopal C, Kumar V (2005) Removal of lead (II) by adsorption using treated granular activated carbon: batch and column studies. *J Hazard Mater* 125:211–220
31. Asuquo E, Martin A, Nzerem P, Siperstein F, Fan X (2017) Adsorption of Cd(II) and Pb(II) ions from aqueous solutions using mesoporous activated carbon adsorbent: equilibrium, kinetics and characterisation studies. *J Environ Chem Eng* 5:679–698
32. Danish M, Hashim R, Rafatullah M, Sulaiman O, Govind AA (2011) Adsorption of Pb(II) ions from aqueous solutions by date bead carbon activated with ZnCl<sub>2</sub>. *clean - soil, air, water* 39:392–399
33. Shekinah P, Kadirvelu K, Kanmani P, Senthilkumar P, Subburam V (2002) Adsorption of lead (II) from aqueous solution by activated carbon prepared from *Eichhornia*. *J Chem Technol Biotechnol* 77:458–464
34. Krishnan KA, Sheela A, Anirudhan TS (2003) Kinetic and equilibrium modeling of liquid-phase adsorption of lead and lead chelates on activated carbons. *J Chem Technol Biotechnol* 78:642–653
35. Yadav SK, Singh DK, Sinha S (2013) Adsorption study of lead(II) onto xanthated date palm trunk: kinetics, isotherm and mechanism. *Desalin Water Treat* 51:6798–6807
36. Pandey PK, Sharma SK, Sami SS (2015) Removal of lead(II) from waste water on zeolite-NaX. *J Environ Chem Eng* 3:2604–2610
37. Govindarao VMH, Froment GF (1986) Voidage profiles in packed beds of spheres. *Chem Eng Sci* 41:533–539. [https://doi.org/10.1016/0009-2509\(86\)87035-X](https://doi.org/10.1016/0009-2509(86)87035-X)
38. R. Chhabra, M.G. Basavaraj, eds., Flow of fluids through granular beds and packed columns, in: Coulson Richardson's Chem. Eng. Vol. 2A Part. Syst. Part. Technol., 6th ed., Butterworth-Heinemann, 2019: pp. 335–386. <https://doi.org/10.1016/b978-0-08-049064-9.50015-1>.
39. Benyahia F, O'Neill KE (2005) Enhanced voidage correlations for packed beds of various particle shapes and sizes. *Part Sci Technol* 23:169–177. <https://doi.org/10.1080/02726350590922242>
40. Wang L, Chen A, Fields K (2000) Arsenic removal from drinking water by ion exchange and activated alumina plants, Cincinnati, Ohio.
41. Bhardwaj V, Kumar P, Singhal G (2014) Toxicity of heavy metals pollutants in textile mills effluents. *Int J Sci Eng Res* 5:664–666
42. Juella D, Vera M, Cruzat C, Alvarez X, Vanegas E (2021) Mathematical modeling and numerical simulation of sulfamethoxazole adsorption onto sugarcane bagasse in a fixed-bed column. *Chemosphere* 280:130687. <https://doi.org/10.1016/j.chemosphere.2021.130687>

43. Danish M, Ansari KB, Aftab RA, Danish M, Zaidi S, Trinh QT (2021) gPROMS-driven modeling and simulation of fixed bed adsorption of heavy metals on a biosorbent: benchmarking and case study. *Environ Sci Pollut Res*. <https://doi.org/10.1007/s11356-021-13207-y>
44. Arim AL, Neves K, Quina MJ, Gando-Ferreira LM (2018) Experimental and mathematical modelling of Cr(III) sorption in fixed-bed column using modified pine bark. *J Clean Prod* 183:272–281. <https://doi.org/10.1016/j.jclepro.2018.02.094>
45. de Freitas GR, Vieira MGA, da Silva MGC (2018) Batch and fixed bed biosorption of copper by acidified algae waste biomass. *Ind Eng Chem Res* 57:11767–11777
46. Sotelo JL, Ovejero G, Rodríguez A, Álvarez S, García J (2012) Removal of atenolol and isoproturon in aqueous solutions by adsorption in a fixed-bed column. *Ind Eng Chem Res* 51:5045–5055
47. Weber TW, Chakravorti RK (1974) Pore and solid diffusion models for fixed-bed adsorbers. *AIChE J* 20:228–238
48. Adeolu AT, Okareh OT, Dada AO (2016) Adsorption of chromium ion from industrial effluent using activated carbon derived from plantain (*Musa paradisiaca*) wastes. *Am J Environ Prot* 4:7–20

**Publisher's note** Springer Nature remains neutral with regard to jurisdictional claims in published maps and institutional affiliations.

Springer Nature or its licensor holds exclusive rights to this article under a publishing agreement with the author(s) or other rightsholder(s); author self-archiving of the accepted manuscript version of this article is solely governed by the terms of such publishing agreement and applicable law.